Novel Highly Fluorinated Poly(arylene ether-1,3,4-oxadiazole)s, Their Preparation, and Sensory Properties to Fluoride Anion

Jianfu Ding* and Michael Day

Institute for Chemical Process and Environmental Technology, National Research Council Canada, 1200 Montreal Road, Ottawa, Ontario, Canada, K1A 0R6

Received May 9, 2006; Revised Manuscript Received July 3, 2006

ABSTRACT: 2,5-Bis(pentafluorophenyl)-1,3,4-oxadiazole (FPOx) has been prepared and successfully polymerized with hexafluorobisphenol A (6F−BPA) by means of an aromatic nucleophilic substitution reaction to produce highly fluorinated poly(arylene ether-1,3,4-oxadiazole)s (FPAEOx). The presence of the highly electron-withdrawing oxadiazole (Ox) group in FPOx significantly enhanced the reactivity of the *p*-fluorine substituents such that the reaction could be completed in only 1−2 h at room temperature in the presence of 4.0 equiv of potassium fluoride (KF). These mild reaction conditions with low reaction temperatures and the use of a mild base effectively prevented side reactions and ensured the formation of polymers with number-average molecular weights up to 64 000 Da free of cross-linking. FPOx itself and this unit in the FPAEOx were found to be capable of selectively binding fluoride anion (F^-) with high affinity, and produced new peaks in UV and fluorescence spectra, which are in new regions and well-isolated from the original peaks of FPOx or the polymer. The intensities of these resulting new peaks corresponded to the fluoride concentrations. All these features make the monomer and the polymer potential candidates for fluoride sensory and enable the detection a high reliability and a high sensitivity to the concentration as low as 0.1 ppm. This sensory system also showed a very high selectivity for detecting F^-, displaying no response to other tested anions including Cl^-, Br^-, ClO_4^-, HSO_4^-, and PF_6^-.

Introduction

The detection of fluoride anions (F^-) is important for a wide range of applications such as medical diagnostics,[1] environmental and chemical processing monitoring,[2] and even chemical warfare agent alerts.[3] Among the several widely used F^- detecting and sensing techniques including electrochemical,[4] colorimetric (UV),[5] and fluorescence responses,[6] UV and fluorescence detections have attracted the most attention since they have been demonstrated high sensitivities with detecting limit as low as sub-ppm (parts per million).[7] These sensitivity levels are frequently required for many applications such as medical diagnostics, drinking water analysis and chemical warfare agent detection. A key component of these UV and fluorescence detectors is the sensory material, which is usually an organic material or polymer containing a build-in chromophore and a fluoride receptor, the latter is usually a functional group being capable of interacting with the fluoride anion. Ideally the receptor should be directly connected to the chromophore in such manner that once the receptor interacts with F^-, it will trigger a specific response in the UV and fluorescence spectra of the chromophore. Currently two types of receptors have been widely used for the interaction with F^-. The first involves a group containing covalently bonded proton such as an aromatic N−H group,[8] which is capable of a strong hydrogen bonding interaction with F^-.[9] The second involves an electron-deficient group[10] such as a boronic group,[4−6] which is able to form a strong Lewis acid−base interaction with F^-. In both cases, to achieve the desired high sensitivity of the UV and fluorescence detection is relied on the structure of the sensory molecules. A strong conjugation of the chromophore with the fluoride receptor is beneficial in enhancing the interaction of the receptor with the F^- and promoting the UV and fluorescence response of the material upon binding F^-.[4−9] On the other hand, because of the strong basic character of F^-, attaching strong electron-withdrawing groups to the receptor will increase the electron deficiency of the receptor and consequently enhance the binding affinity with F^-.[11] A major problem with many of the current UV and florescence based fluoride sensory materials is their poor selectivity, since they frequently have positive responses to some other anions such as Cl^-, $H_2PO_4^-$, and Br^-. In addition, most of them only produce intensity changes in UV and fluorescence spectra upon binding. The result based on intensity change alone is much less reliable and less sensitive than one in which the detection is based on the formation of completely new peaks located at different wavelengths in the spectra once binding has occurred.

Poly(ether-1,3,4-oxadiazole)s represent a class of materials that combine outstanding mechanical and electrical properties, high thermal and chemical stability with special functionalities such as high electron affinity[12] associated with the existence of the highly electron-deficient oxadiazole (Ox) rings in the polymer chain. While the majority of this type of materials are used as high performance engineering materials in application areas such as aerospace,[13] some have been found applications as anion sensory and electron-transporting materials.[14,15] In the case the C−H bonds on the aromatic main chain of the polymer have been replaced by C−F bonds, such as reported in the present study, the strong electron-withdrawing effect of the C−F bonds on the perfluorophenyl rings adjacent to the Ox units in the polymer is anticipated to further enhance the electron-deficient property of the Ox unit, so that to have a certain interaction with fluoride anion.[11]

Traditionally, poly(ether-1,3,4-oxadiazole)s were prepared through polyhydrazide using a ring closing reaction.[12−15] However, attempts to prepare polyhydrazides from the condensation reaction of a diacid and a hydrazine also produced some multisubstituted structures of the hydrazide unit as side reactions. These multisubstituted hydrazide units were not able to form

* Corresponding author. jianfu.ding@nrc-cnrc.gc.ca.

10.1021/ma061043o CCC: $33.50 Published 2006 by the American Chemical Society
Published on Web 08/11/2006

Scheme 1. Reaction Scheme for the Preparation of FPAEOx Using S_NAr Reaction of FPOx with 6F−BPA

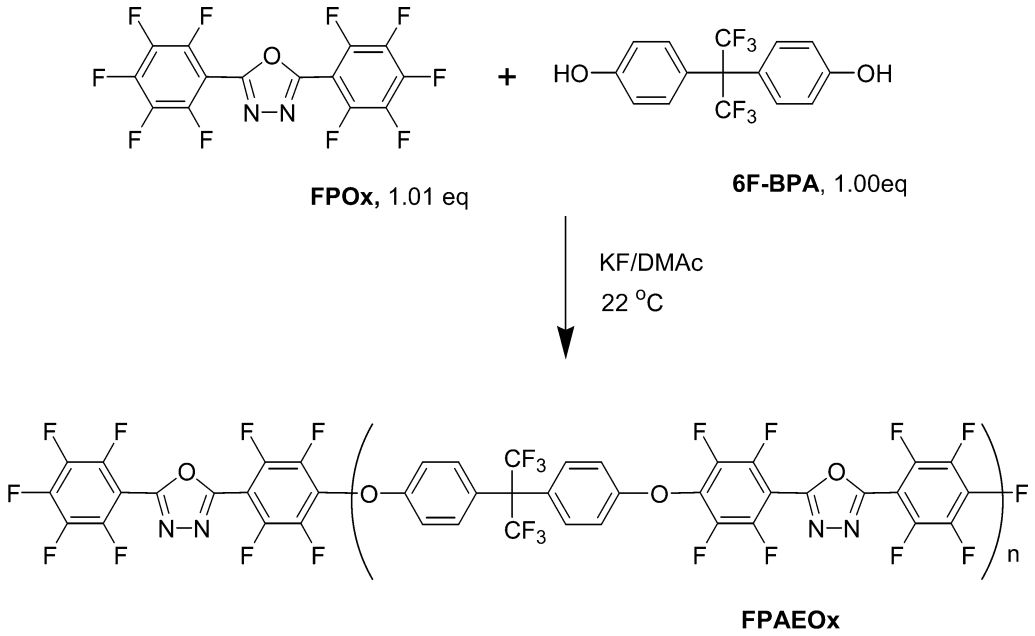

oxadiazole rings in the subsequent ring closing reaction. Consequently the poly(ether-1,3,4-oxadiazole)s prepared using this approach contained a certain amount of defects. An alternative method that is capable of avoiding this drawback involves the S_NAr substitution of an Ox containing dihalide compound such as 2,5-bis(fluorophenyl)-1,3,4-oxadiazole with a bisphenol. However, the Ox ring in the monomer is usually sensitive to nucleophilic attacking and as such is not stable under the traditional S_NAr reaction conditions for preparing conventional polyethers.[16] Fortunately, we found that bis(pentafluorophenyl) monomers such as bis(pentafluorophenyl)sulfone and bis(pentafluorophenyl) ketone are much more reactive for the S_NAr reaction than corresponding difluoride due to the extra activating effect of the additional C−F bonds on the phenyl rings in the monomers.[17] As a consequence the reaction of bis(pentafluorophenyl) monomers with hexafluorobisphenol A (6F−BPA) could be performed under very mild reaction conditions. For instance, the reaction between bis(pentafluorophenyl) sulfone and 6F−BPA can be completed in a few hours at 35 °C in the presence of 2.1 equiv of KF. It is well-known that the Ox group is also a strong electron-withdrawing group and has a comparable activating effect to the S_NAr reactions as sulfone and ketone groups;[18] thus, FPOx should permit the reaction to be done at similar mild reaction conditions. By the use of such mild reaction conditions, it is now possible for the Ox unit to have sufficient stability to allow the polymerization to complete, such that high molecular weight polymers have been prepared with well-defined linear chain structures similar to those reported for the analogue ketone and sulfone polymers.[17]

Results and Discussions

1. Polycondensation between FPOx and 6F—BPA. The difference in the molecular structures of FPOx with bis(pentafluorophenyl) sulfone is that the sulfone linkage in the latter has been replaced by a Ox unit, which has a comparable electron-withdrawing effect. Consequently, FPOx is expected to have a similar reactivity in the S_NAr polycondensation reaction with 6F−BPA. This allows for the use of a mild polymerization condition. Briefly, FPOx and 6F−BPA in a feed molar ratio of 1.01/1.00 were reacted in DMAc at room temperature (RT) in the presence of KF (Scheme 1). The reactions were monitored using ^{19}F NMR, and the results are shown in Figure 1.

^{19}F NMR measurements have clearly indicated that FPOx is indeed more reactive than the analogue sulfone and ketone monomers, allowing the reaction to be completed in a short time (1−2 h) at a low temperature (22 °C), producing a high molecular weight polymer. The ^{19}F NMR spectra in Figure 1 clearly demonstrate the loss of the *p*-C−F bonds of FPOx, indicating the formation of the polymer and cyclic oligomers during the reaction. The signal of the $-CF_3$ in 6F−BPA at −63.80 ppm (not shown) is shifted slightly to −63.74 ppm as it is incorporated into the polymer. Because the total amount of $-CF_3$ during the reaction remained unchanged, this peak was therefore used as an internal standard for the quantitative analysis. Examination of Figure 1 reveals that the sample at 0 min has three peaks at −136.70, −148.64, and −161.39 ppm in the aromatic range, which are assigned to the *o*-, *p*-, and *m*-fluorine substituents of the FPOx. As the reaction proceeded, the intensities of these three peaks decreased, meanwhile two new peaks appeared at −136.85 and −153.44 ppm and increased in intensity with reaction time. These two new peaks are assigned to the *o*- and *m*-fluorine substituents (relative to the Ox groups) on the FPOx units in the polymer main chain. Meanwhile, the peaks associated with the pentafluorophenyl units at the chain ends remained at the same position as those of the free FPOx. Examination of the spectrum of the 60 min sample reveals the presence of only two peaks in aromatic region, which were associated with the main chain fluorines. It is only when the signal is magnified by 20-fold that the very weak peaks associated with the pentafluorophenyl end group become apparent as shown in the inset of Figure 1. This result indicates that a high molecular weight polymer with a well-defined linear structure could be produced. The conversion of each sample (p) at different reaction time can be obtained by comparing the integral peak intensities of the corresponding fluorine substituents on the main chain with those at the chain ends. Considering the feed ratio (r_0) of 1.01 for this reaction, we are able to calculate the number-average

CDV

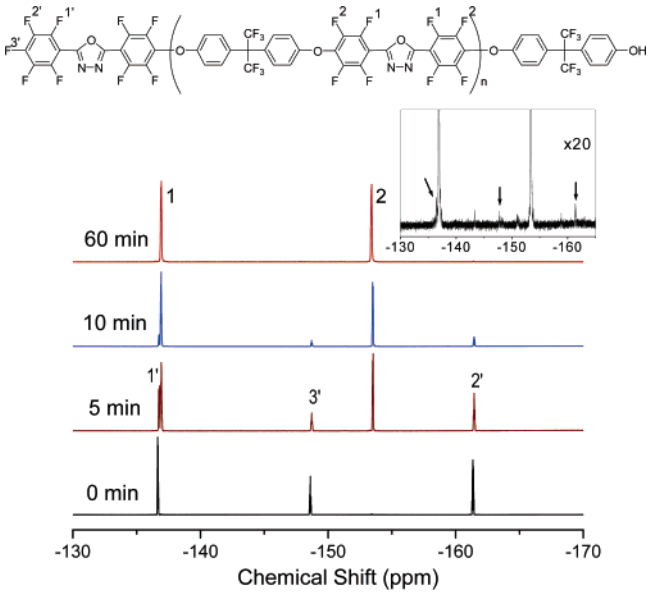

Figure 1. ^{19}F NMR spectra of the samples taken at 0, 5, 10, and 60 min from the reaction of FPOx with 6F−BPA in DMAc in the presence of 4.0 equiv of KF at 22 °C. The solution sample was directly mixed with acetone-d_6 for the analysis after filtration to remove the insoluble solid. The peak assignments are indicated in the inset chemical structure of the polymer. The spectrum of the 60 min sample has been magnified in intensity in order to identify the weak signals in the background.

Table 1. Thermal Properties of FPAEOx with Different Molecular Weights

M_n/kDa[a]	M_w/M_n	Tg (°C)	$T_d^{5\%}$ (°C)
2.66 (2.33)	1.65	125	n/d
2.94 (3.00)	1.60	132	n/d
5.75 (5.05)	1.65	149	430
7.16 (7.61)	1.68	158	n/d
12.8 (11.7)	1.67	168	475
25.2 (22.5)	1.75	175	n/d
31.5 (38.0)	1.80	177	480
64.0 (58.0)	2.50	179	480

[a] The molecular weights were determined by GPC with the columns calibrated using polystyrene standards. The values in the brackets were calculated from the ^{19}F NMR spectra base on the end group analysis using eq 1.

molecular weight (M_n) of each sample using eq 1.[19] (See Table 1)

$$M_n = \frac{M_0(r_0 + 1)}{2r_0(1 - p) + (1 - r_0)} \quad (1)$$

where M_0 is the mass of the repeat unit of the polymer.

Meanwhile, the portion of the solution sample for GPC and ^{1}H NMR analyses was purified by dropping into water to precipitate the polymer. Once dried the polymer was dissolved in $CDCl_3$ for ^{1}H NMR measurement and in THF for GPC analysis. The ^{1}H NMR spectra of samples taken at 0, 5, 10, and 60 min are shown in Figure 2. In the case of the initial sample (0 min), two double peaks at 7.23 and 6.83 ppm and a single peak at 6.57 ppm are clearly evident and can be attributed to the *m*- and *o*-protons (relative to the isopropyl unit) and the phenol group of 6F−BPA. As the formation of the ether linkage, the peaks of these two protons on phenyl ring shifted to lower field and each of them separated to three double peaks, which are ascribable to the phenyl units inside the main chain, that next to the end phenol group and end phenol group itself as indicated in the inset chemical structure of Figure 2. The

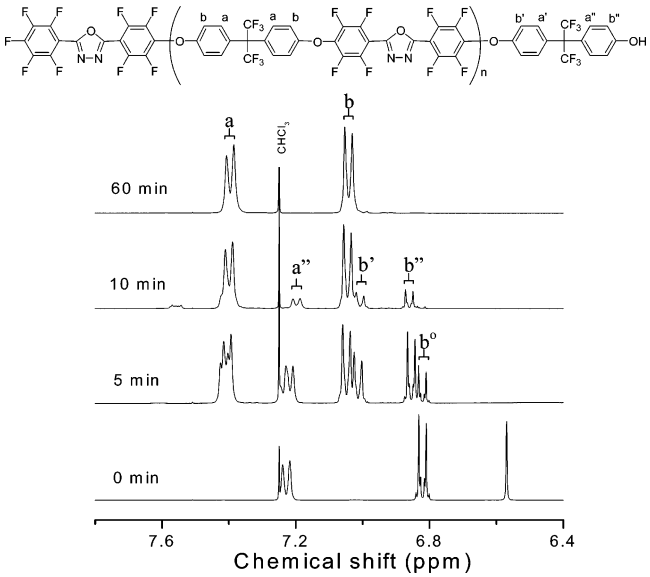

Figure 2. ^{1}H NMR spectra of the same samples as for Figure 1. The samples were purified by precipitating the solution into water/methanol (80/20) and dried as described in experimental, prior to the spectrum being recorded in $CDCl_3$.

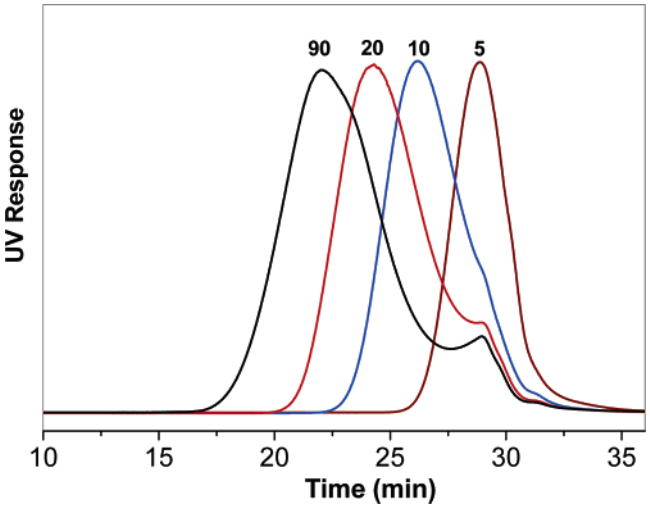

Figure 3. GPC curves of the samples taken from the reaction of FPOx with 6F−BPA in DMAc in the presence of 4.0 equiv of KF at 22 °C at 5, 10, 20, and 90 min. Samples were purified by dropping the solution into water/methanol (80/20) mixture so that both polymer and oligomer were collected.

resulting final polymer (60 min) only showed two double peaks at 7.40 and 7.05 ppm related to the two different protons of the 6F−BPA units in the main chain, indicating a high molecular weight of the final product. This result is consistent with that from ^{19}F NMR measurement. However, due to the much higher resolution and signal/noise ratio of ^{19}F NMR spectra, only the data from ^{19}F NMR spectra was used for number-average molecular weight (M_n) calculation for the samples at different reaction times.

The GPC curves of the samples taken at 5, 10, 20, and 90 min are displayed in Figure 3. To minimize errors associated with the loss of any material during polymer purification, the solution sample was precipitated into water (containing 20% methanol) to ensure that polymer in the whole molecular weight range was recovered. Using this approach the cyclic oligomers were also included in the sample, the cyclic oligomers were statistically produced from the polycondensation reaction with the content dependent on the concentration of the reactants.[20]

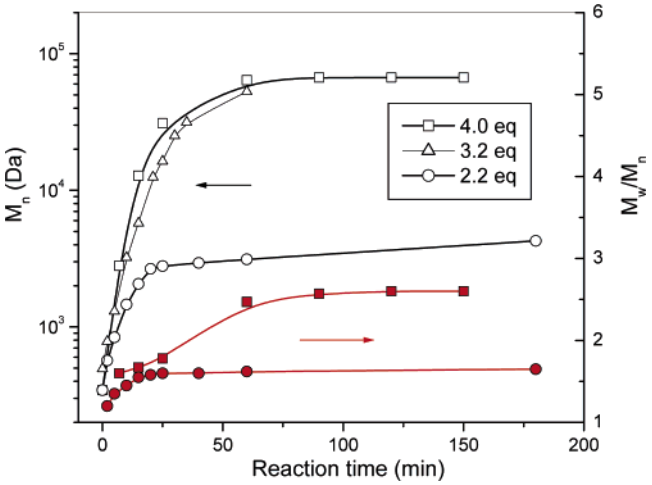

Figure 4. Variation of the molecular weight and molecular weight distribution as a function of reaction time for the polymers produced from the polycondensation of FPOx with 6F−BPA in the presence of different amount of KF (2.2, 3.2, and 4.0 equiv) in DMAc at 22 °C with a feed ratio of FPOx/6F−BPA = 1.01/1.00.

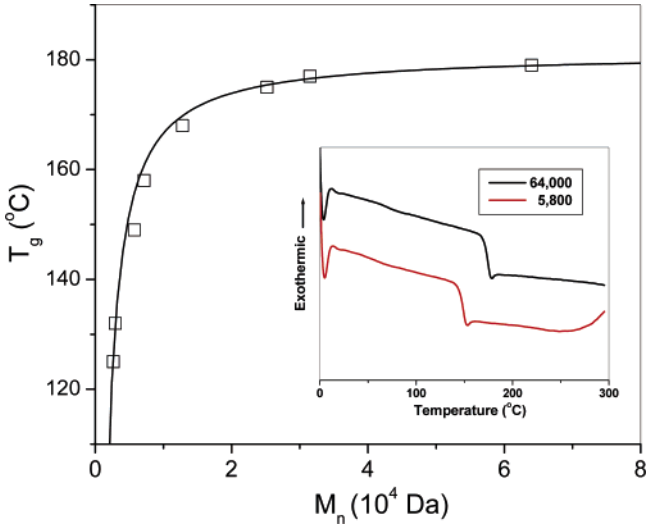

Figure 5. Variation of the glass transition temperature of FPAEOx as a function of molecular weight (M_n). The solid line represents the best fitting curve obtained by the use of the Fox equation ($T_g = T_g^\infty - K/M_n$), which gave values of $T_g^\infty = 181.2$ °C, and $K = 1.46 \times 10^4$ °C·Da. Inset: DSC curves of polymers with molecular weight of 64 000 ($T_g = 179$ °C), and 5800 Da ($T_g = 149$ °C).

The presence of the cyclic oligomers is readily visible by a small peak centered around 29 min, which shows no noticeable change in the position and intensity with the reaction time. The consistency of these data suggested that the cyclic oligomers were mainly formed in the early stages of the reaction, where the two ends of a short single chain had a greater chance to meet each other for cyclization. Once the oligomers have formed, they became inert to further polymerization. Therefore, in the polymer molecular weight calculation, the contribution of the oligomer peak to GPC curves was removed using a peak resolving technique, and the calculated molecular weights and molecular weight distributions of the polymers as a function of reaction times were presented in Figure 4. The values of M_n calculated from GPC and NMR measurements were also compared in Table 1, which showed that the values from the GPC measurement are slightly higher than the corresponding values from the end group analysis using NMR. The higher rigidity of the FPAEOx chain than that of polystyrene standards used for GPC calibration produced a larger coil size of FPAEOx in the solution and resulted in a larger apparent molecular weight from the GPC measurement. Therefore, M_n from the NMR measurement should be more close to the real value.

2. The Effect of KF on the Polycondensation. As described in our previous paper for the reaction between bis(pantafluorophenyl) sulfone and 6F−BPA,[17c] KF in this type of polycondensation reaction acts both as a catalyst to activate 6F−BPA by converting phenol to phenoxide, and as a base to neutralize HF by forming a KHF_2 complex. Consequently, a little more than 2.0 equiv (relative to 6F−BPA) of KF was sufficient to complete the reaction. However, it was found that the use of 2.2 equiv of KF for the reaction of FPOx with 6F−BPA in DMAc at 22 °C only produced an oligomer with a molecular weight of ~3000 Da (Figure 4), corresponding to a conversion of ~90% for the reaction. Increasing reaction time in this case did not help to increase the final conversion of the reaction. This observation would appear that the reaction equilibrium has been established under this reaction condition. Only when the amount of KF is increased to 3.2 equiv, this equilibrium was removed to allow the molecular weight of the polymer to grow to 53 000 Da in 60 min. A further increase in the amount of KF to 4.0 equiv, however, only slightly increased the rate of reaction and had no apparent effect to the molecular weight of the final polymer. This result suggests that 3.2 equiv of KF is essentially required to complete the reaction. It is about 1 equiv of KF more than that required for the reactions of the analogue ketone and sulfone monomers.[17] Therefore, there must be a specific interaction occurred between KF and the Ox group in this reaction, which is tying up 1 equiv of KF during the reaction.

Examination of Figure 4 clearly indicates that the reaction was almost complete in 60 min. Extending the reaction time did not significantly promote the molecular weight nor had any effect on the quality of the polymer, indicating no side reactions occurred under this reaction condition. This represents a significant progress by comparing within the traditional polycondensation reaction of bis(pentafluorophenyl) monomer with 6F−BPA at high temperatures, in which polymer quality usually degraded during the prolonged reaction time due to side reactions of the *o*-fluorine substituents of the perfluorophenyl unit in the polymer.[17,21] These side reactions would lead to branched and even cross-linked polymer structures. In addition, they would also break the balance between *p*-fluorine substituents and phenol groups in the feeding. All these effects have been shown to cause wide molecular weight distributions along with lower number-average molecular weights of the polymers. In extreme situations, cross-linked polymer gels are formed during the reaction. The GPC analysis (Figure 3) and the reaction kinetic analysis (Figure 4) indicated that this reaction at low temperature is superior to the conventional S_NAr polycondensation reaction of bis(pentafluorophenyl) monomers with 6F−BPA in terms of improved selectivity of the reaction to the *p*-fluorine substituents in the monomer.

3. Thermal Properties of the Polymer. DSC analysis of the polymers with different molecular weights showed a typical glass transition as displayed in the inset of Figure 5. No crystalline related transitions were found in the temperature range from 0 to 300 °C. The effect of molecular weight on the glass transition temperature (T_g) has been plotted in Figure 5. It can be seen that the T_g monotonically increases with molecular weight, with the curve leveling off when the molecular weight (M_n) exceeds 30 000 Da. The data of T_g as a function of M_n can be fitted by the Fox equation ($T_g = T_g^\infty - K/M_n$) to give the solid line shown in Figure 5,[22] reflecting the character of

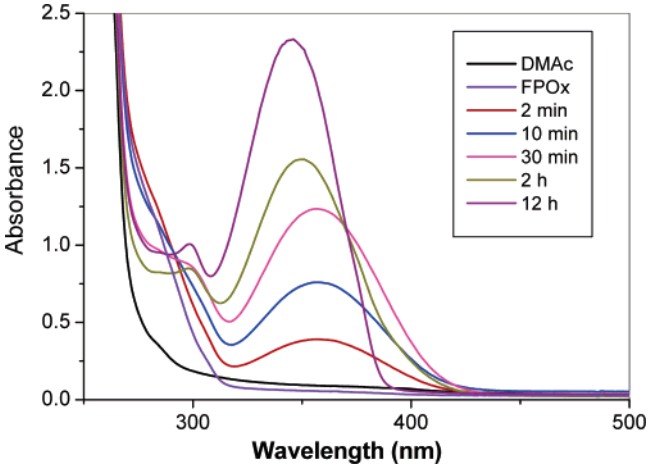

Figure 6. UV−vis spectra of FPOx solutions in DMAc (0.08 mM) obtained after various periods of time following the addition of solid KF at room temperature.

the linear polymer chain. From this fitting curve the glass transition temperature of the polymer with infinite molecular weight, T_g^∞ of 181.2 °C can be derived along with the Fox constant, K, of 1.46×10^5. While the molecular weight has a significant influence to the T_g, its effect on the decomposition temperature is less significant. For example, the high molecular weight polymer (M_n = 64 000 Da) had a 5% weight loss temperature ($T_d^{5\%}$) of 480 °C, while the $T_d^{5\%}$ of the polymer with M_n = 12 500 Da was only 5 °C lower. These values are comparable to those observed for the analogous sulfone polymer.[17c] It should also be noted that the DSC curve of the low molecular weight sample (inset of Figure 5) displayed an exothermic transition starting at 250 °C. This transition is believed to be due to a further condensation reaction between the unconsumed phenol and *p*-fluorine end groups occurred at the high temperature. In this case, the polymer with a M_n of 5800 Da contains about 10% of the original reactive phenol groups and *p*-fluorine substituents from the starting material as the chain ends. This part of phenol groups and *p*-fluorine substituents is easily reacted each other at the temperature higher than 250 °C.[23] This reaction has also produce a response in the TGA analysis, in which ~2% weight loss has been observed in the temperatures range from 250 to 350 °C. This weight loss corresponds to the release of HF during the thermal condensation reaction.

4. The Interaction between FPOx and KF. The interaction between FPOx and KF was investigated using UV−vis spectrometry. In this investigation, approximately 5 mg of KF (0.1 mmol) was added to 3 mL of FPOx solution (0.08 mM) in DMAc in an UV cuvette. The UV spectra of the solution were then measured as a function of time and the results are displayed in Figure 6. It can be seen that the absorption edge of the pure solvent is around 280 nm, while the shoulder peak of the FPOx solution at around 290 nm should be attributable to the absorption of FPOx. Once solid KF was added to the solution, a new peak centered around 355 nm gradually appeared and increased in intensity during the whole 12 h testing period. Meanwhile the shoulder peak at 290 nm decreased in intensity. This phenomenon suggests that interaction between FPOx and KF is occurring. However, it is worth to note that this process is slow and appears to reach completion in about 12 h. This slow interaction rate may be due to the extremely low solubility of KF in DMAc. If it is the case, the addition of a highly soluble fluoride should result in a much faster response, a fact that will be verified later in the discussions. On the other hand, the following observations provide some insight into the mechanism of this interaction. (1) Similar responses were found for other fluorides including NaF, KF, RbF, CsF, and Bu_4NF. (2) No UV changes were observed with other anionic salts including Cl^-, Br^-, HSO_4^-, ClO_4^-, and PF_6^-. On the basis of these observations it would appear that this UV response is caused by a specific interaction between FPOx and F^-. It therefore is likely that perfluorinated structure of the phenyl ring in FPOx is strongly withdrawing electrons out of the Ox ring, making it extremely electron deficient, such that it is capable of producing a strong Lewis acid−base interaction with F^-. Similar interactions with F^- have been observed with some Lewis acids, which have been used for the detection of F^- in solution.[4−6,10] Aromatic rings attached with strong electron withdrawing groups such as nitro and cyano are usually found to be sufficiently electron deficient as a soft Lewis acid to interact with a soft Lewis base.[24] Though in some case the formed complex is not stable enough to be isolated, many of these interactions caused changes in UV spectra upon the formation of the complex.[24b] In FPOx, the Ox ring becomes highly electron deficient due to strong electron withdrawing effect of the multiple fluorine substituents. The presence of the two pyridine-type nitrogens in the Ox aromatic ring further enhanced this effect and made the Ox ring even higher electron deficient. The pyridine-type nitrogen was usually found promoting the electron depletion of the π-orbit of the ring (p 651 of ref 24b). All of these effects introduced some hard Lewis acid feature to the Ox ring in this molecule. Therefore, it is likely that the interaction site with F^- is the Ox ring.

5. F^- Sensory Property of FPOx. As a consequence of these observations it would appear that FPOx has the potential to be an excellent sensing material for detecting F^- in solution with good selectivity. However, based upon the data presented in Figure 6, it is clear that the interaction of FPOx with KF in DMAc is slow and as such is not ideal for a sensing application. However, as already pointed out, this observed slow interaction may be due to the extremely low solubility of solid KF in the DMAc solution. To confirm this assumption, a highly soluble fluoride, tetrabutylammonium fluoride (Bu_4NF) was examined. This involved preparing a series of DMAc solutions with a fixed concentration of FPOx (0.03 mM) and a varied concentration of Bu_4NF in a range from 0.0045 to 4.5 mM. Interestingly, the addition of Bu_4NF into the FPOx solution produced an immediate change in the UV spectra of the solutions. Furthermore, the changes in the spectra were largely depended on the concentration of Bu_4NF as show in Figure 7. The original solution of FPOx (0.03 mM) only has one peak at 280 nm (black curve). When a trace amount of Bu_4NF was added into the solution, a new absorption peak at 358 nm immediately appeared. The intensity of this peak increased in a nearly linear manner with the increase of Bu_4NF concentration in the range from 0.0045 to 0.135 mM. This concentration range corresponds to 0.1 to 2.6 ppm of fluoride anion. At the concentration of 0.135 mM, this peak appeared to reach saturation and then decreased slightly in intensity with further increases of the F^- concentration. However, at this point in the concentration profile, another new peak appeared at 443 nm, which gradually increased in intensity with the concentration increased from 0.045 to 1.35 mM. This behavior of the successive formation of multiple absorption peaks upon the increase of F^- concentration suggested multiple F^- binding to FPOx. The titration curve for the peak at 358 nm as shown in the inset of Figure 7 has been analyzed using Benesi−Hildebrand equation.[25] The result indicated that a reversible 1:1 complex could be formed in the

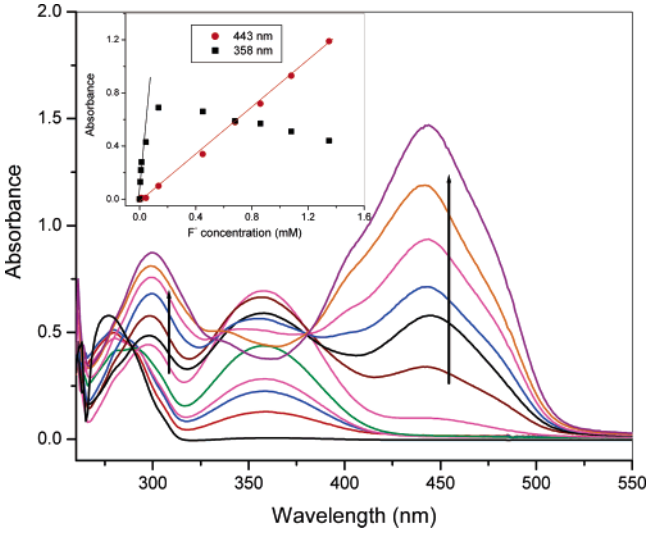

Figure 7. UV spectra of FPOx in DMAc (0.03 mM) following the addition of Bu_4NF with different concentrations of the solution at room temperature. The spectra were obtained by subtracting the solvent background. The inset displayed the variation of the peak intensities at 358 and 443 nm with the fluoride concentration.

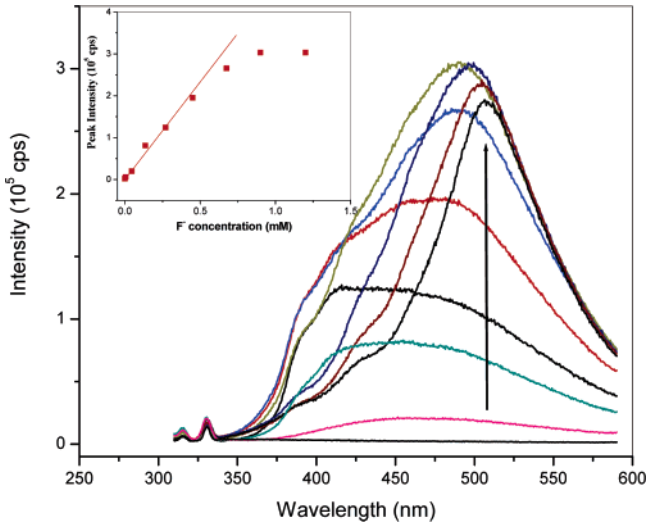

Figure 8. Fluorescent emission spectra of FPOx solution in DMAc (0.03 mM), to which Bu_4NF of different concentrations have been added. The inset represented the peak intensity varied with the fluoride concentration.

low F^- concentration region with a binding constant of 52 000 M^{-1} (see Supporting Information).

Meanwhile, it was noted that FPOx also showed a very sensitive fluorescence response to fluoride anion as displayed in Figure 8. The pure FPOx solution in DMAc displayed two weak and narrow emission peaks at 316 and 331 nm when excited at 300 nm. As soon as Bu_4NF was added to this solution, a strong and broad fluorescence emission band at around 450 nm appeared. This band gradually increased in intensity as the concentration of Bu_4NF increased from 0.045 to 1.20 mM, while the two original peaks remained unchanged in the position and intensity. In addition it was also noted that this broad fluorescence emission peak was gradually red-shifted and became slightly narrower as the F^- concentration increased. The plot of peak intensity as a function of the F^- concentration (inset in Figure 8) showed a linear relationship in the range from 0.0045 to 0.45 mM. However, at F^- concentrations greater than 1.20 mM, there was no longer increase in peak intensity with concentration. This result suggests that the fluorescence measurements can be used in a similar manner as UV measurement for detecting F^-. On the basis of these observations it is clear that FPOx as a F^- sensory material for UV and fluorescence detection offers a significant advantage over many other systems, due to the fact that the sensing response is based on the new-formed UV and fluorescence peaks at the wavelengths where no any overlapping with the signals of the original molecule was founded. This property ensures a high reliability for qualitative and quantitative detecting.[6c] Furthermore, the results of a test for some other anions presented in Figure 9 indicated that FPOx has a very high selectivity in sensing F^-. When Bu_4NClO_4, Bu_4NHSO_4, Bu_4NPF_6, Bu_4NBr, Bu_4NCl, and Bu_4NF were individually added to the FPOx solutions (0.03 mM) at a concentration of 2.2 mM, Bu_4NF was the only species to generate a special fluorescence emission. All the other salts did not produce any change in fluorescence spectrum compared to that of the pure FPOx solution.

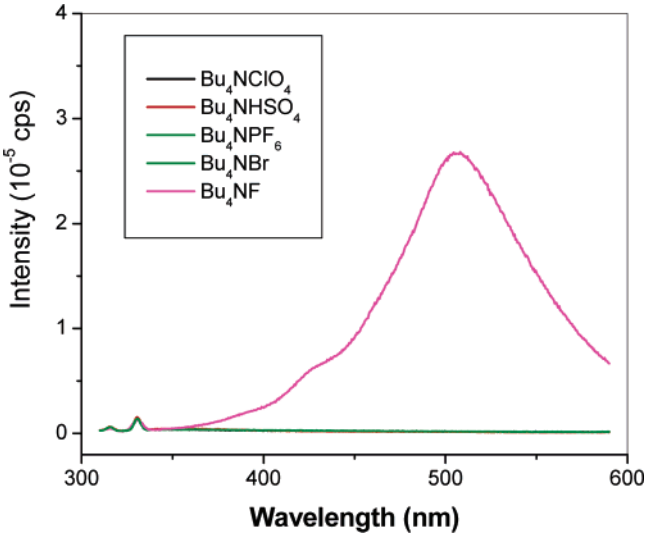

Figure 9. Fluorescence spectra of FPOx solution in DMAc in the presence of different anions. The concentration of FPOx was 0.03 mM, and the concentration of the tetrabutylammonium salt was 2.2 mM.

6. F^- Sensory Property of FPAEOx. In addition to the excellent F^- sensory properties of FPOx in terms of its high sensitivity and selectivity for both UV and fluorescence detection, the polymers containing FPOx units are also of interests due to some additional attributes. For example, the larger conjugated structures and the higher potential of the interaction between the active units of the polymers in some case enabled the polymer a signal amplifying capability in fluorescence detection.[26] Therefore, the F^- sensory property of the FPOx-containing polymer, FPAEOx has also been tested in two different solvents, namely DMAc and acetonitrile. The influence of different concentrations of Bu_4NF on the fluorescence spectra of FPAEOx is shown in Figure 10, which indicated that the pure polymer solution in DMAc displayed a very strong peak at 363 nm, in addition to a narrow weak peak at 331 nm. The latter is at the same position as noted for the FPOx monomer as shown in Figure 8. A much higher emission intensity of this peak than that observed for the FPOx monomer is clearly evident, and will be beneficial to offer an improved sensitivity of the detection. Figure 10 shows that the intensity of this strong peak is very sensitive to the presence of small amount of fluoride anion in solution. For example when Bu_4NF is added to the pure polymer solution (0.03 mM) at a concentration of 0.0045 mM, the intensity of this peak decreased about 10%. More importantly, a new peak at 454 nm formed at the same time. The intensities of both peaks changed with the fluoride

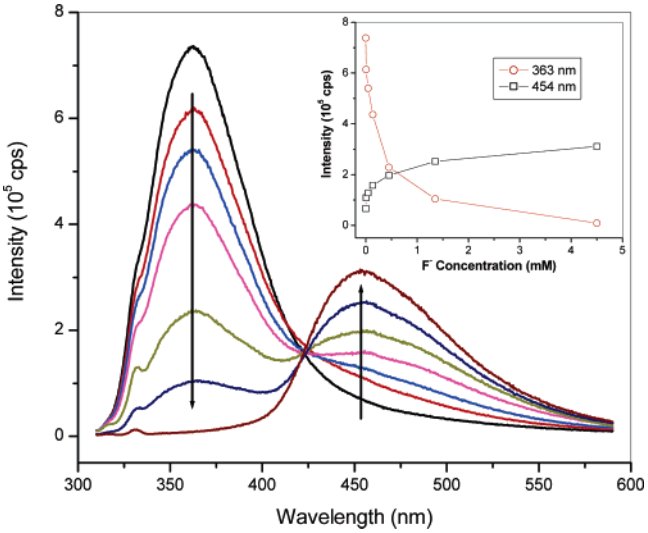

Figure 10. Fluorescence spectra of FPAEOx solution in DMAc, to which Bu_4NF of different concentrations have been added. The concentration of the polymer was 0.03 mM (based on repeat unit).

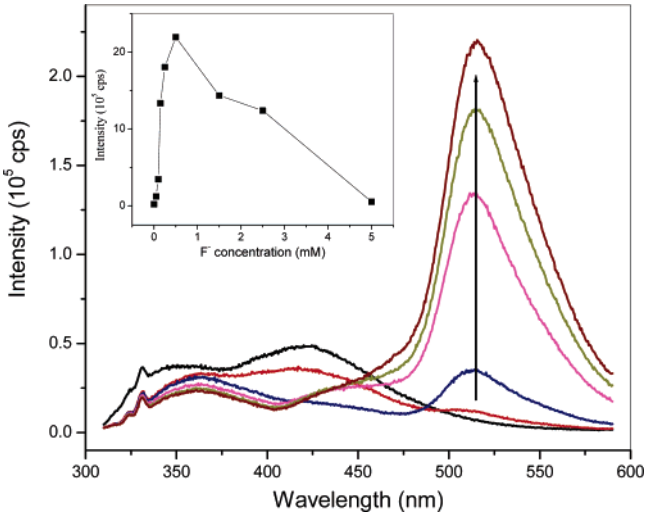

Figure 11. Fluorescence spectra of FPAEOx solution in acetonitrile, to which Bu_4NF of different concentrations have been added. The concentration of the polymer in the solution was about 0.005 mM based upon the calculation from UV measurements.

concentration. The plots of the intensity as a function of the concentration are shown in the inset of Figure 10, which displayed a monotonically decrease of the intensity of the peak at 363 nm with the fluoride concentration following a nearly first order exponential decay relationship. Meanwhile, the intensity of the peak at 454 nm follows a nearly first order exponential growth. These exponential relationships for both peaks are capable of providing high detection sensitivity to the very low concentrations, meanwhile maintaining a wide effective detecting concentration range, consequently to achieve an optimized performance of the sensory devices. Analysis of the titration curve from the emission band at 363 nm using a 1:1 complex model described by Conners confirmed a reversible 1:1 complex formed in the solution in a low F^- concentration region from 0.0045 to 1.35 mM (See Supporting Information).[25] However, the complex from the polymer has a lower binding constant (4440 M^{-1}) than that from the monomer.

The sensory property was also tested using acetonitrile as the solvent. However, acetonitrile is a poor solvent for the polymer. Though a solution with 0.03 mM concentration was intended to prepare, only part of the polymer was dissolved in the solvent. The real concentration of the resulting solution is estimated by UV measurement being 0.005 mM. The fluorescence spectra obtained in acetonitrile solution are presented in Figure 11, from which it can be seen that the solution of pure polymer only has a very weak emission in a broad range from 300 to 500 nm. However the addition of Bu_4NF to the solution resulted in the formation of a new strong peak at 515 nm. The intensity of this peak increased rapidly from a value of almost 0 at a fluoride concentration of about 0.0135 mM to its highest value at 0.5 mM, clearly indicating a high sensitivity to the concentration change over this range. However, the sensitivity of this detection to the low fluoride concentration is not as good as the polymer in DMAc. The new peak at 515 nm did not apparently appear until the fluoride concentration reached 0.0135 mM, while the polymer in DMAc solution showed an obvious response when the fluoride concentration is 3 times lower. This phenomenon is in contrary with what was expected. Because the polymer concentration in this solution is much lower, the interaction of the FPOx units in the polymer with F^- should be saturated at a lower F^- concentration. Therefore, a higher sensitivity of the detection to low fluoride concentration should be achieved. This low sensitivity to low F^- concentration is probably caused by the poor solubility of the polymer. As displayed in Figure 11, the pure FPAEOx solution in acetonitrile did not show a strong peak at ~363 nm as observed in DMAc, rather a very broad band in a very wide range from 300 to 500 nm, suggesting aggregations of the FPOx units in the polymer is probably occurring. This aggregation could quench the fluorescence from polymer and produced a broad emission band, which overlapped with the new formed emission upon the addition of fluoride anion, consequently interfered the detection of the weak fluorescence signals produced at low fluoride concentrations. In this situation, the new signal only can be detected when the fluoride concentration is high enough to produce the signal with intensity greater than that of the aggregation emission. This phenomenon suggested that any aggregation of FPOx units in the sensory materials should be avoided in order to ensure high detection sensitivity to the low concentrations.

Experimental Section

Instrumentation. Nuclear magnetic resonance spectra were recorded using a Varian Unity Inova spectrometer at a resonance frequency of 400 MHz for ^1H, and 376 MHz for ^{19}F. $CDCl_3$ was used as the solvent for the final product analysis, while acetone-d_6 was used as the solvent for the kinetic analysis of the polymerization by ^{19}F NMR. The $-CF_3$ peak of FPOx at -63.8 ppm was used as an internal standard for the molecular weight calculation. Molecular weights were also determined by gel permeation chromatography (GPC) using a Waters 515 HPLC pump, coupled with a Waters 410 differential refractometer detector and a Waters 996 photodiode array detector operating at a wavelength of 260 nm. A set of MicroStyragel columns (10^3, 10^4, and 10^5 Å) was used for polymer analysis, and another set of MicroStyragel columns (100, 500, 1000 Å) was used for the oligomer analysis. These columns were calibrated using a set of polystyrene standards in THF. UV−vis absorption spectra were recorded on a Hewlett-Packard 8453 spectrometer. Fluorescence emission spectra were obtained with a Spex Fluorolog 3 spectrometer. The differential scanning calorimetry (DSC) analysis and the thermogravimetric analysis (TGA) were performed under a nitrogen atmosphere (60 mL/min) on TA Instruments DSC 2920 and TGA 2950, respectively, at a heating rate of 10 °C/min. The melting point (MP) was presented with a temperature range from onset to peak position. The FT-IR spectra were recorded on a Midac M1200-SP3 spectrophotometer by using a diamond cell for the monomer sample, and a film for polymer sample. MS data was obtained using a Prince (Prince Technologies,

The Netherlands) capillary electrophoresis system coupled to an API3000 mass spectrometer (Applied Biosystems/Sciex, Concord) via a microspray interface. A sheath solution of 1 uL/min. 2-propanol/methanol (2:1) was used, with 30 mM ammonium acetate dichloromethane/methanol (3:1) as the running buffer.

Materials. Anhydrous DMAc, acetonitrile (spectrophotometric grade) were purchased from Sigma-Aldrich Ltd and used as received. 6F−BPA was purified by recrystallization from toluene. Pentafluorobenzoic acid was purchased from Oakwood Products Inc and was used without any purification. The other chemicals and reagents were used as received.

Preparation of 2,5-Bis(pentafluorophenyl)-1,3,4-oxadiazole (FPOx). Pentafluorobenzoic acid (52.1 g, 0.246 mol) and hydrazine sulfate (19.5 g, 0.150 mol) were added into 450 g of polyphosphoric acid in a round-bottom flask, which was equipped with a magnetic stirrer and a condenser. The reaction system was then evacuated and filled with argon for three times to remove air and moisture. The solution was heated to 150 °C with stirring under the protection of argon and maintained at this temperature for 1 h, and then the reaction temperature was slowly increased to 200 °C over 1 h. The solution was allowed to further react for an additional hour at this temperature until no more gas release was observed. The reaction solution was then cooled to about 50 °C and poured into 2 L of distilled water with stirring. The white precipitate was collected by filtration and washed with hot water until the filtrate was neutral. The dried crude product was then recrystallized from a toluene/2-propanol (30/70) mixture twice, producing 40.5 g of the pure product with a yield of 82%. MP: 156.2−157.4 °C. ^{19}F NMR (δ, $CDCl_3$): 63.80 (s, CF_3), 134.33 (m, 4F ortho to Ox), 145.10 (m, 2F, para to Ox), 158.39 (m, 4F, meta to Ox). MS: 403.2 (MH^+); calcd for $C_{14}F_{10}N_2O$, 402.15. Anal. Calcd: C, 41.81; F, 47.24; N, 6.97; O, 3.98. Found: C, 41.14; N, 6.83. FT-IR (diamond window): 1655 (C═N of Ox ring), 1565, 1506, 1424, 1367, 1323, 1218, 1100, 1042, 993, 845, 824, 782, 751, 711 cm^{-1}.

Polymerization of FPOx with 6F—BPA. FPOx (0.608 g, 1.51 mmol) and 6F−BPA (0.504 g, 1.50 mmol) were added to 8 mL of anhydrous DMAc in a test tube. Then, 0.2 mL of aliquot was taken as the 0 min sample for analysis. To the stirred solution was added 0.349 g of KF (6.00 mmol). The mixture was then stirred at room temperature (22 °C) with 0.2 mL of aliquots being taken at desired times for NMR and GPC analysis. Each sample was filtered through a Kimwipes plug in a dropping pipet to remove insoluble salts. Because the solvent, DMAc does not produce any signals in the ^{19}F NMR spectra, the solution sample was analyzed without purification. Therefore, 0.05 mL of the filtered solution was then added to a NMR tube containing 0.5 mL of acetone-d_6 for ^{19}F NMR measurement. The remaining filtrate was dropped into 5 mL of a mixture of water/methanol (80/20, v/v) to precipitate the organic material, which was collected, washed with water, and dried under vacuum prior to ^{1}H NMR and GPC analysis. The final reaction solution was filtered and dropped into 100 mL of methanol to precipitate the polymer, which was further washed with methanol three times prior to being dried to produce the final product, FPAEOx. ^{19}F NMR (δ, $CDCl_3$): 63.80 (s $-CF_3$), 134.80 (m, 4F ortho to Ox), 150.76 (m, 4F, meta to Ox). ^{1}H NMR (δ, $CDCl_3$): 7.40 (d, *J* 8.8 Hz, 4H), 7.04 (d, *J* 8.8 Hz, 4H). FT-IR (film): 1653 (C═N of Ox ring), 1607, 1510, 1482, 1228 (ether), 1177, 994, 930, 853 cm^{-1}. Anal. Calcd for [$C_{29}H_8F_{14}N_2O_3$], repeat unit: C, 49.88; H, 1.15; F, 38.09; N, 4.01; O, 6.87. Found: C, 48.93; H, 1.08; N, 3.98.

Conclusion

The polycondensation of FPOx with 6F−BPA can be easily conducted at room temperature in DMAc in the presence of KF to produce polymers with high molecular weights and well-defined linear chain structures. During the reaction, KF not only acts as a catalyst and as a base as found for other bis-(pentafluorophenyl) monomers, but also interacts with oxadiazole group in FPOx unit. This interaction consumed additional 1 equiv of KF. Therefore, compared to the reaction of other bis(pentafluorophenyl) monomers, the reaction of FPOx required 1 equiv more KF so that the reaction can be completed. This interaction was confirmed by UV studies, which revealed a new strong absorption in the spectrum upon the addition of KF into the FPOx solution. This change in the UV spectrum upon the addition of KF has been further investigated to determine the possible use of FPOx as a sensory material for the detection of fluoride anion in solution. The results of this investigation suggest that this molecule has a very high sensitivity and selectivity in both UV and fluorescence detection for sensing fluoride anion with a lower detection limit of about 0.1 ppm. The FPOx-containing polymer, FPAEOx, showed a similar sensitivity and selectivity in sensing fluoride anion in both DMAc and acetonitrile solutions. However, due to the poor solubility, the polymer in actonitrile showed a tendency of aggregation of the FPOx unit, which caused a lower sensitivity to the solution with low fluoride concentrations, (i.e., concentrations lower than 0.0135 mM).

Supporting Information Available: Text giving the titration isotherm plot analysis and figures showing the variation of the peak intensities at 358 nm, the variation of the peak intensities at 363 nm, and FT-IR spectra of FPOx and FPAEOx. This material is available free of charge via the Internet at http://pubs.acs.org.

References and Notes

(1) Kirk, K. L. *Biochemistry of the Halogens and Inorganic Halides*; Plenum Press: New York, 1991.
(2) Direisbuch, R. H. *Handbook of Poisoning*; Lange Medical Publishers: Los Altos, CA, 1980.
(3) (a) Sohn, H.; Létant, S.; Sailor, M. J.; Trogler, W. C. *J. Am. Chem. Soc.* **2000**, *122*, 5399. (b) Zhang, S.-W.; Swager, T. M. *J. Am. Chem. Soc.* **2003**, *125*, 3420.
(4) Nicolas, M.; Fabre, B.; Simonet, J. *Chem. Commun.* **1999**, 1881.
(5) (a) Solé, S.; Gabbaï, F. *Chem. Commun.* **2004**, 1284. (b) Cho, E. J.; Ryu, J.; Lee, Y. J.; Nam, K. C. *Org. Lett.* **2005**, *7*, 2607. (c) Yamamoto, H.; Ori, A.; Ueda, K.; Dusemund, C.; Shinkai, S. *Chem. Commun.* **1996**, 407.
(6) (a) Melaimi, M.; Gabbaï, F. *J. Am. Chem. Soc.* **2005**, *127*, 9680. (b) Cooper, C. R.; Spencer, N.; James, T. D. *Chem. Commun.* **1998**, 1365. (c) Neumann, T.; Dienes, Y.; Baumgartner, T. *Org. Lett.* **2006**, *8*, 485.
(7) (a) Anzenbacher, P. Jr.; Jursiková, K.; Sessler, J. L. *J. Am. Chem. Soc.* **2000**, *122*, 9350. (b) Badr, I. H. A.; Meyerhoff, M. E. *J. Am. Chem. Soc.* **2005**, *127*, 5318. (c) Yamaguchi, S.; Akiyama, S.; Tamao, K. *J. Am. Chem. Soc.* **2001**, *123*, 11372.
(8) (a) Boiocchi, M.; Boca, L. D.; Gomez, D. E.; Fabbrizzi, L.; Licchelli, M.; Monzani, E. *J. Am. Chem. Soc.* **2004**, *126*, 16507. (b) Jose, D. A.; Kumar, D. K.; Ganguly, B.; Das, A. *Org. Lett.* **2004**, *6*, 3445. (c) Yun, S.; Ihm, H.; Kim, H. G.; Lee, C. W.; Indrajit, B.; Oh, K. S.; Gong, Y. J.; Lee, J. W.; Yoon, J.; Lee, H. C.; Kim, K. S. *J. Org. Chem.* **2003**, *68*, 2467. (e) Esteban-Gómez, D.; Fabbrizzi, L.; Licchelli, M. *J. Org. Chem.* **2005**, *70*, 5717.
(9) (a) Mizuno, T.; Wei, W.-H.; Eller, L. R.; Sessler, J. L. *J. Am. Chem. Soc.* **2002**, *124*, 1134. (b) Sessler, J. L.; Maeda, H.; Mizuno, T.; Lynch, V. M.; Furuta; H. *J. Am. Chem. Soc.* **2002**, *124*, 13474. (c) Miyaji, H.; Sato, W.; Sessler, J. L. *Angew. Chem., Int. Ed.* **2002**, *39*, 1777. (d) Anzenbacher, P., Jr.; Jursíková, K.; Lynch, V. M.; Gale, P. A.; Sessler, J. L. *J. Am. Chem. Soc.* **1999**, *121*. 11020. (e) Black, C. B.; Andrioletti, B.; Try, A. C.; Ruiperez, C.; Sessler, J. L. *J. Am. Chem. Soc.* **1999**, *121*, 10438.
(10) (a) Martinez-Manez, R.; Sancenon, F. *Chem. Rev.* **2003**, *103*, 4419. (b) Yamaguchi, S.; Akiyama, S.; Tamao, K. *J. Am. Chem. Soc.* **2000**, *122*, 6793. (c) Aldridge, S.; Bresner, C.; Falls, I. A.; Coles, S. J.; Hursthouse, M. B. *Chem. Commun.* **2002**, 740.
(11) (a) Nishiyabu, R.; Anzenbacher, P., Jr. *J. Am. Chem. Soc.* **2005**, *127*, 8270. (b) Nishiyabu, R.; Anzenbacher, P., Jr. *Org. Lett.* **2006**, *8*, 359. (c) Tong, H.; Wang, L.; Jing, X.; Wang, F. *Macromolecules* **2003**, *36*, 2584.
(12) (a) Gomes, D.; Borges, C.; Pinto, J. C. *Polymer* **2004**, *45*, 4997. (b) Hsiao, S.-H.; Chiou, J.-H. *J. Polym. Sci., Part A: Polym. Chem.* **2001**, *39* 2271. (c) Maglio, G.; Palumbo, R.; Tortora, M.; Trifuoggi, M.; Varricchio, G. *Polymer* **1998**, *39*, 6407.
(13) Bottino, F. A.; Di Pasquale, G.; Iannelli, P. *Macromolecules* **2001**, *34*, 33.

(14) (a) Zhou, G.; Cheng, Y.; Wang, L.; Jing, X.; Wang, F. *Macromolecules* **2005**, *38*, 2148. (b) Tong, H.; Zhou, G.; Wang, L.; Jing, X.; Wang, F.; Zhang, J. *Tetrahedron Lett.* **2003**, *44*, 131.
(15) Chochos, C. L.; Govaris, G. K.; Kakali, F.; Yiannoulis, P.; Kallitsis, J. K.; Gregoriou, V. G. *Polymer* **2005**, *46*, 4654.
(16) (a) Labadie, J. W.; Hedrick, J. L. *Macromolecules* **1990**, *23*, 5371. (b) Atwood, T. E.; Newton, A. B.; Rose, J. B. *Br. Polym. J.* **1972**, *4*, 391. (c) Chung, I. S.; Kim, S. Y. *J. Am. Chem. Soc.* **2001**, *123*, 11071. (d) Hedrick, J. L. *Macromolecules* **1991**, *24*, 812.
(17) (a) Ding, J.; Liu, F.; Li, M.; Day, M.; Zhou, M. *J. Polym. Sci., Part A, Polym. Chem.* **2002**, *40*, 4205. (b) Ding, J.; Day, M.; Robertson, G. P.; Roovers, J. *Macromol. Chem. Phys.* **2004**, *205*, 1070. (c) Ding, J.; Qi, Y.; Day, M.; Jiang, J.; Callender, C. L. *Macromol. Chem. Phys.* **2005**, *206*, 2396.
(18) (a) Johnson, R. N.; Farnham, A. G.; Clendinning, R. A.; Hale, W. F.; Merriam, C. N. *J. Polym. Polym. Sci., Part A-1* **1967**, *5*, 2375. (b) Carter, K. R. *Macromolecules* **1995**, *28*, 6462. (c) Lozano, A. E.; Jimeno, M. L.; de Abajo, J.; de la Campa, J. G. *Macromolecules* **1994**, *27*, 7164−7170.
(19) Elias, Hans-Georg. *Macromolecules 2, Synthesis and Materials*; Stafford, John W., translator; Plenum Press: New York, 1977; p 599.
(20) Chen, M.; Gibson, H. W. *Macromolecules* **1996**, *29*, 5502. (b) Kricheldorf, H. R.; Böhme, S.; Schwarz, G.; Krüger, R.-P.; Schulz, G. *Macromolecules* **2001**, *34*, 8886. (c) Baxter, I.; Williams, D. J.; Ben-Haida, A.; Hodge, P.; Kohnke, F. H.; Colquhoun, H. M. *Chem. Commun.* **1998**, 2213.
(21) Kimura, K.; Tabuchi, Y.; Yamashita, Y.; Cassidy, P. E.; Fitch, J. W., III; Okumura, Y. *Polym. Adv. Technol.* **2000**, *11*, 757.
(22) Rudin, A. *The Elements of Polymer Science and Engineering*; Academic Press: New York, 1982; p 401.
(23) (a) Attwod, T. E.; King, D. A.; Newton, A. B.; Rose, J. B. *Polymer* **1977**, *18*, 359. (b) Rao, V. L. *J. Macromol. Sci.—Rev. Macromol. Chem. Phys.* **1999**, *C39*, 655.
(24) For review, see: (a) Smith, M. B.; March, J. *March's Advanced Organic Chemistry, Reactions, Mechanisms, and Structure*; John Wiley & Sons: New York, 2001; pp 104 and 342. (b) Melby, L. R. In *The Chemistry of the Cyano Group*; Rappoport, Z., Ed.; Interscience Publishers: New York, 1970; p 639. (c) Jensen, W. B. *The Lewis Acid−Base Concepts, An Overview*; Interscience Publishers: New York, 1980; pp 112−155.
(25) (a) Conners, K. A. *Binding Constants: The Measurement of Molecular Complex Stability*; John Wiley & Sons: New York, 1987. (b) Benesi, H.; Hildebrand, J. H. *J. Am. Chem. Soc.* **1949**, *71*, 2703. (c) Black, C. B.; Andrioletti, B.; Try, A. C.; Ruiperez, C.; Sessler, J. L. *J. Am. Chem. Soc.* **1999**, *121*, 10438.
(26) (a) McQuade, D. Y.; Pullen, A. E.; Swager, T. M. *Chem. Rev.* **2000**, *100*, 2527. (b) Saxena, A.; Fujiki, M.; Rai, R.; Kim, S.-Y.; Kwak, G. *Macromol. Rapid Commun.* **2004**, *25*, 1771.

MA061043O